Materials Today Bio 22 (2023) 100791

Contents lists available at ScienceDirect

Materials Today Bio

journal homepage: www.journals.elsevier.com/materials-today-bio

Microencapsulated stem cells reduce cartilage damage in a material dependent manner following minimally invasive intra-articular injection in an OA rat model

Castro Johnbosco [a,1], Lisanne Karbaat [a,1], Nicoline M. Korthagen [b,c,1], Kelly Warmink [c], Michelle Koerselman [a], Katja Coeleveld [d], Malin Becker [a], Bas van Loo [a], Bram Zoetebier [a], Sanne Both [a], Harrie Weinans [c], Marcel Karperien [a,2,*], Jeroen Leijten [a,2,**]

[a] Department of Developmental BioEngineering, TechMed Centre, University of Twente, the Netherlands
[b] Faculty of Veterinary Sciences Department of equine sciences, University of Utrecht, the Netherlands
[c] Department of Orthopaedics, University Medical Centre Utrecht, the Netherlands
[d] Department of Rheumatology & Clinical Immunology, University Medical Centre Utrecht, the Netherlands

ARTICLE INFO

Keywords:
Microencapsulation
Micromaterials
Stem cells
Biomaterials

ABSTRACT

Osteoarthritis (OA) is a degenerative disease of the joints for which no curative treatment exists. Intra-articular injection of stem cells is explored as a regenerative approach, but rapid clearance of cells from the injection site limits the therapeutic outcome. Microencapsulation of mesenchymal stem cells (MSCs) can extend the retention time of MSCs, but the outcomes of the few studies currently performed are conflicting. We hypothesize that the composition of the micromaterial's shell plays a deciding factor in the treatment outcome of intra-articular MSC injection. To this end, we microencapsulate MSCs using droplet microfluidic generators in flow-focus mode using various polymers and polymer concentrations. We demonstrate that polymer composition and concentration potently alter the metabolic activity as well as the secretome of MSCs. Moreover, while microencapsulation consistently prolongs the retention time of MSC injected in rat joints, distinct biodistribution within the joint is demonstrated for the various microgel formulations. Furthermore, intra-articular injections of pristine and microencapsulated MSC in OA rat joints show a strong material-dependent effect on the reduction of cartilage degradation and matrix loss. Collectively, this study highlights that micromaterial composition and concentration are key deciding factors for the therapeutic outcome of intra-articular injections of microencapsulated stem cells to treat degenerative joint diseases.

1. Introduction

Stem cell therapy has the potential to revolutionize our capacity to treat traumatic injury [1–3], pathological tissue damage [4–6], and age-related degeneration of tissues [7–9]. Owing to their regenerative potential, stem cells are positioned as a key cell source for tissue engineering strategies [10]. Although much research has focused on the multi-lineage differentiation capacity of mesenchymal stem cells (MSCs) to form tissues, emerging evidence suggests that MSCs regenerative potential is, at least in part, mediated via secretion of trophic factors such as exosomes [11], cytokines [12], and growth factors [13]. Indeed, many of these factors are well-known for their immunomodulatory and pleiotropic effects, which can guide tissue regeneration [14]. Although animal models have shown promising therapeutic effects following MSC injections for various applications [15,16], the therapeutic effectivity of all explored MSC treatments is currently hindered by their rapid in vivo clearance [17].

Osteoarthritis is a chronic inflammatory and cartilage degenerative joint disease. Contemporary treatment of osteoarthritis is mostly palliative, and no curative treatment currently exists [18,19]. Consequently,

* Corresponding author.
** Corresponding author.
E-mail addresses: marcel.karperien@utwente.nl (M. Karperien), jeroen.leijten@utwente.nl (J. Leijten).
[1] CJ, LK, and NMK are shared lead authors; the authorship sequence is randomly determined and may be adjusted for CV purposes.
[2] JL and MK are shared corresponding authors.

https://doi.org/10.1016/j.mtbio.2023.100791
Received 13 June 2023; Received in revised form 5 August 2023; Accepted 4 September 2023
Available online 7 September 2023

novel therapeutic modalities to modify, slow-down, or cure osteoarthritis are urgently needed. To this end, intra-articular injection of MSCs has recently been pioneered to treat OA [20,21]. In line with other envisioned MSC treatments, intra-articular injection of MSCs associates with both promising results and a rapid clearance of injected cells, which effectively reduced its therapeutic window and subsequent therapeutic effect [22–24]. Intra-articularly injected cells are cleared by the immune system and egression from the joint space possibly via the semi-porous synovial lining [25].

Hence, microencapsulation of stem cells in micrometer-sized hydrogels (e.g., microgels) is anticipated as a key method to protect implanted or injected cells, prolonging in vivo retention, and widening the therapeutic window, thus potentially boosting treatment outcomes [26–28]. Moreover, biomaterial-based encapsulation determines the fate of stem cells by tuning the material' bio-physical and mechanical properties [29,30]. Specifically, encapsulated MSCs in a biomaterial microenvironment when injected into cartilage defects promote chondrogenesis by differentiating into chondrocytes minimizing further cartilage damage [31,32]. However, the pioneering studies that investigated the effect of intra-articularly injected microencapsulated cells on joint health have reported inconsistent outcomes. Specifically, while extension to in vivo, retention has been universally observed, therapeutic outcomes have varied from no additional beneficial effect to reduced cartilage damage [33]. Notably, none of these studies has investigated the effect of distinct material compositions on treatment outcomes [34,35]. Cell-material interactions can potently steer stem cell behavior by controlling cell morphology, shape, volume, and aggregation [36], truly based on biomaterial properties such as stiffness, degradability, and matrix remodeling which further induce phenotypical alterations [37] and promote tissue regeneration [38]. Hence, we hypothesized that the selection of biomaterial for microencapsulation could therefore play a determining role in the outcome of intra-articularly injected microencapsulated stem cells using biomaterials.

Various biomaterials such as alginate and GelMA have been investigated for the encapsulation of cells. However, identified that only a few studies investigated the intra-articular injection of cell-laden microgels [39,40]. Hence, we investigated whether material composition could influence cell behavior, and in particular its effect on retention capability and therapeutic outcome. However, dextran and hyaluronic acid-based hydrogels as injectable materials are highly cytocompatible [41], have easily tunable biophysical properties, and are available in clinical grade [42], which are currently under clinical investigation. Being modified with tyramine moieties, they can be crosslinked on-chip by the proven enzymatic crosslinking method which is highly superior, orthogonal, and faster than other crosslinking methods [43–45] and can be universally expanded to other different materials. Hence, we leveraged microfluidic droplet generation microdevices to produce highly controlled stem cell-laden microgels made of dexTA and dexHATA for intra-articular injection. To compare cell-material dependency on therapeutic effects of the MSCs, we produced distinct microgel formulations that controllably varied in their composition, formulation, and size. Following in vitro characterization, the distinctly formulated stem cell-microgels were intra-articularly injected in the synovial joint space of healthy rats to study cell retention. Furthermore, the therapeutic effects of the distinct stem cell-laden microgels were studied in a rat OA model using a whole joint analysis approach. Together, this study represents the most complete analysis in terms of material selection, microparticle production, biological characterization, and in vivo implantation which revealed that material selection and formulation are key determinant factors of cellular behavior and therapeutic outcome of intra-articularly injected stem cells. Selecting, tuning, and modifying injectable material systems provides an operational and theoretical framework to facilitate the translation of stem cells into an effective osteoarthritis treatment.

2. Result & discussion

2.1. Microfluidic production of tuneable stem cell-laden microgels

To produce stem cell-laden microgels of distinct biomaterials, dextran-tyramine conjugates (dexTA) and hyaluronic acid-tyramine conjugates (HATA) were synthesized [46]. For dexTA, the hydroxyl groups of Dextran were activated with 4-nitrophenyl chloroformate (PNC) and subsequent amination via the addition of an excess of tyramine (TA), which yielded a dexTA conjugate with a degree of substitution (DS) of 10% confirmed with ^{1}H NMR with DS defined as % of modified monosaccharide units (S1.a). Subsequently, HATA conjugates were prepared by activating the COOH groups of hyaluronic acid with DMTMM, which showed higher levels of amination than carbodiimide chemistry was confirmed with ^{1}H NMR to yield a 3.4% degree of substitution of TA moieties (S1.b) with DS defined as % of modified disaccharide units. Enzyme-mediated oxidative crosslinking of phenolic moieties (e.g., TA) was leveraged to form microgels using flow-focusing droplet generators in dripping mode to create discrete human bone marrow-derived stromal cell (MSC)-laden polymer droplets, which were on-chip crosslinked as described previously [43] (Fig. 1a–c). Microgels were formed with two distinct formulations: a bioinert formulation composed of dexTA 10w/v%, and a bioresponsive formulation of 10w/v % dexHATA composed of (5 w/v% dexTA and 5 w/v% HATA). The rationale behind choosing such a distinct polymer concentration in dexHATA microgel is to see how such a formulation would have a combinatorial effect on the overall therapeutic effect of cell-laden microgels in vivo. The diameter of the formed microdroplets could be controllably tuned by varying the respective flow rates of the intermittent aqueous phase and the continuous oil phase (Fig. 1d). Both dexTA and dexHATA type microgels could be produced in a monodispersed manner, being described by a coefficient of variation of $<$5% (Fig. 1e) and an average diameter of 105 $\pm$ 7,9 μm for dexTA and 132.5 $\pm$ 9,3 μm for dexHATA microgels (Fig. 1f). Mechanical characterization of crosslinked microgels via optical interferometry-based nanoindentation revealed that dexTA microgels and dexHATA microgels were characterized by a Young's Modulus of 3.65 $\pm$ 0.73 kPa and 1.76 $\pm$ 1.03 kPa, respectively (Fig. 1g). This indicated that blending dexTA with HATA resulted in slightly softer microgels as compared to microgels solely composed of dexTA. Scanning electron microscopy confirmed that MSCs were fully encapsulated as no cellular protrusion could be observed (Fig. 1h) Moreover, fluorescent microscopy of MSC-laden microgels in which the nuclei, cytoskeleton, and TA-TA bonds were fluorescently visualized revealed that the MSCs were randomly distributed throughout the microgels in a dispersed manner (Fig. 1i). Regardless, both types of microgels were associated with high cell viability ($>$90%) shortly after production and in long-term culture (Fig. 1j) Fluorescence quantification of microencapsulated cells revealed that the number of MSCs per microgel remained constant over a culture period of four weeks, which demonstrated the inability of MSCs to egress out of their microgel (Fig. 1k). Together, this confirmed that microencapsulation of MSCs could be achieved in a safe and cell-friendly manner, which effectively prevented the escape and subsequent loss of MSCs for a prolonged period, thereby representing a biomaterial platform technology potentially suited to prolong MSC retention following intra-articular injection of cells for therapeutic applications.

2.2. Polymer content of MSC-laden microgels mediates cellular activity and in vivo retention

We next investigated whether the polymer concentration would affect the function and performance of the produced microgels, and its effect on in vivo retention in particular. To this end, dexTA was chosen due to its bio-inert nature. DexTA of 5w/v% as previously described [47] showed cellular aggregate formation and 10w/v% polymer concentration hypothesized to influence cellular function was chosen as polymer

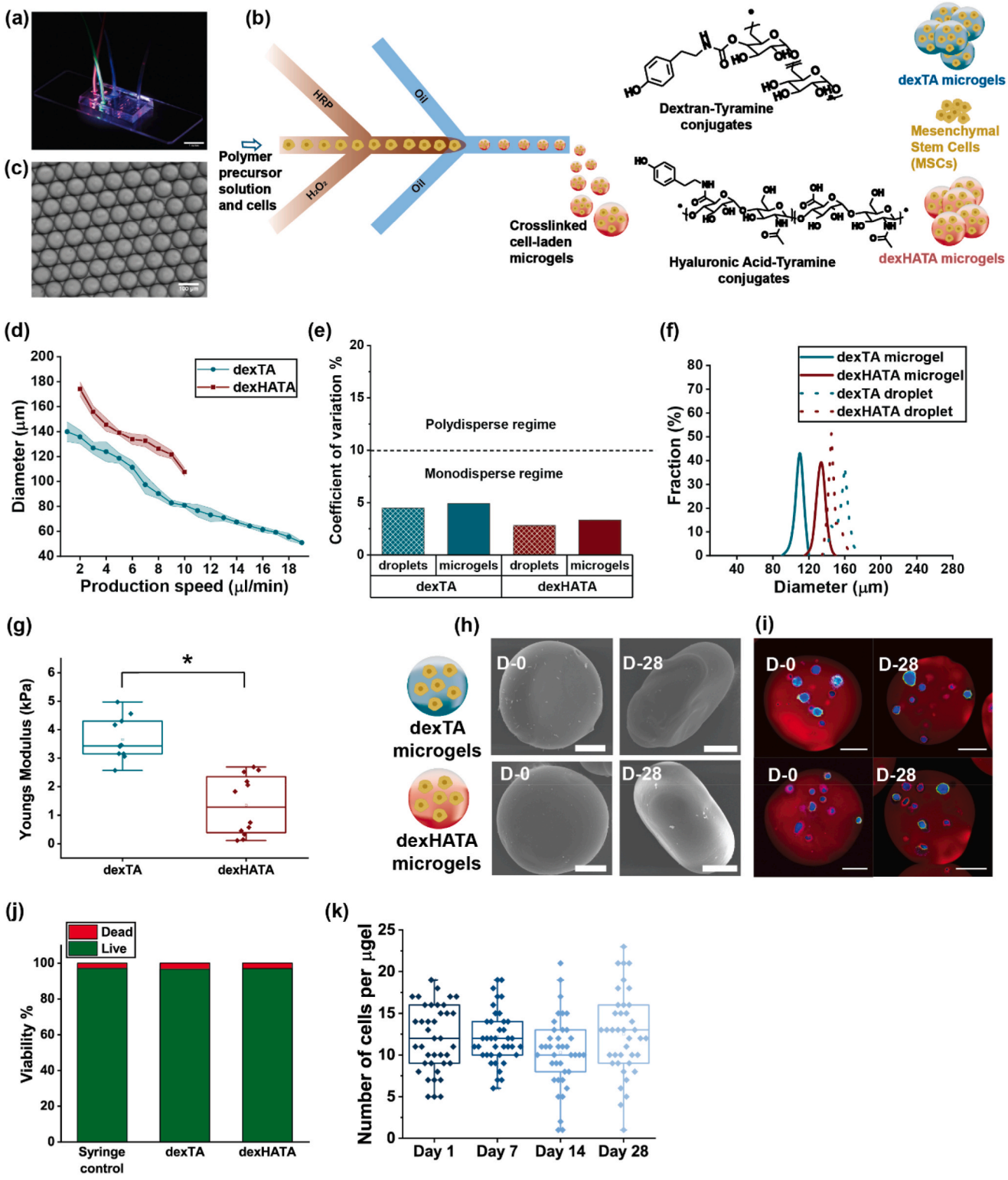

Fig. 1. Microencapsulation of MSCs in dexTA or dexHATA microgels allows for long-term maintenance of cell viability in vitro. **(a)** Photograph and **(b)** schematic of microfluidic chip with connectors used for scalable production of enzymatically crosslinked dexTA or dexHATA microgels. **(c)** Brightfield micrographs of microfluidically produced dexTA microgels. **(d)** Microgel diameter depends on the flow rate and material properties of the polymer precursor ($n > 10$). **(e)** Coefficient of variation of droplets and microgels based on quantification of bright field micrographs ($n > 19$). **(f)** Diameter distribution of dexTA, dexHATA microgels, and droplets ($n \geq 11$). **(g)** Young's Modulus of dexTA and dexHATA microgels based on interferometry-based optical fiber-top nanoindentation ($n > 10$). **(h)** Scanning electron micrographs of MSC-laden microgels after 1 and 28 days. Scale bars equal 50 μm. **(i)** Fluorescent confocal images of dexTA and dexHATA microgels after 1 and 28 days of culture (red: microgels, green: F-actin, and blue: nuclei). Scale bars equal 50 μm. **(j)** Viability of MSCs microencapsulated in dexTA or dexHATA microgels after 14 days. **(k)** Quantification of the number of cells residing in dexTA microgels over 28 days ($n > 39$). Graphical data is represented as mean ± standard deviation. Statistical significance was determined by One-Way ANOVA (*$p < 0.05$).

precursor concentrations to produce MSC-laden microgels. However, other polymer concentrations <2.5w/v% showed in ability to form microgels and >15w/v% had fewer monodispersed microgels (increase in viscosity altered droplet formation). Notably, currently reported studies on intra-articular injection of microencapsulated stem cells have only focused on a single polymer concentration [48]. To explore the effect of this variable, we produced MSC-laden microgels composed of either 5w/v% or 10w/v% dexTA. The difference in diameter between the two compositions was minimal (Fig. 2a). Both microgel compositions could be produced in a monodisperse manner with a coefficient of variation of <5% (Fig. 2b), and the diameter of both compositions could be controlled via the disperse flow speed in comparable manner (Fig. 2c). The young's modulus between two types of microgels was not significantly different (Fig. 2d). However, MSCs microencapsulated in microgels composed of 10w/v% dexTA were characterized by a higher metabolic activity indicating that the cells were able to respond differently to the two distinct compositions (Fig. 2e). We next investigated whether the distinct formulations would affect the in vivo response and the MSC retention time in particular. Histological analysis revealed that some of the injected microgels were able to line or penetrate synovial tissue and that microgels composed of 10w/v% dexTA contained a higher number of cells than 5w/v% dexTA microgels (Fig. 2f). To confirm whether microencapsulation would extent the MSC's retention time, near-infrared labeled microgels were intra-articularly injected, and analyzed after 1, 7, and 15 weeks. This revealed that 10w/v% dexTA microgels offered substantially longer MSC retention time than their 5w/v% dexTA counterparts, with signal half-lives of 2.9 and 5.8 weeks, respectively (Fig. 2g and h). Collectively, these findings confirmed that

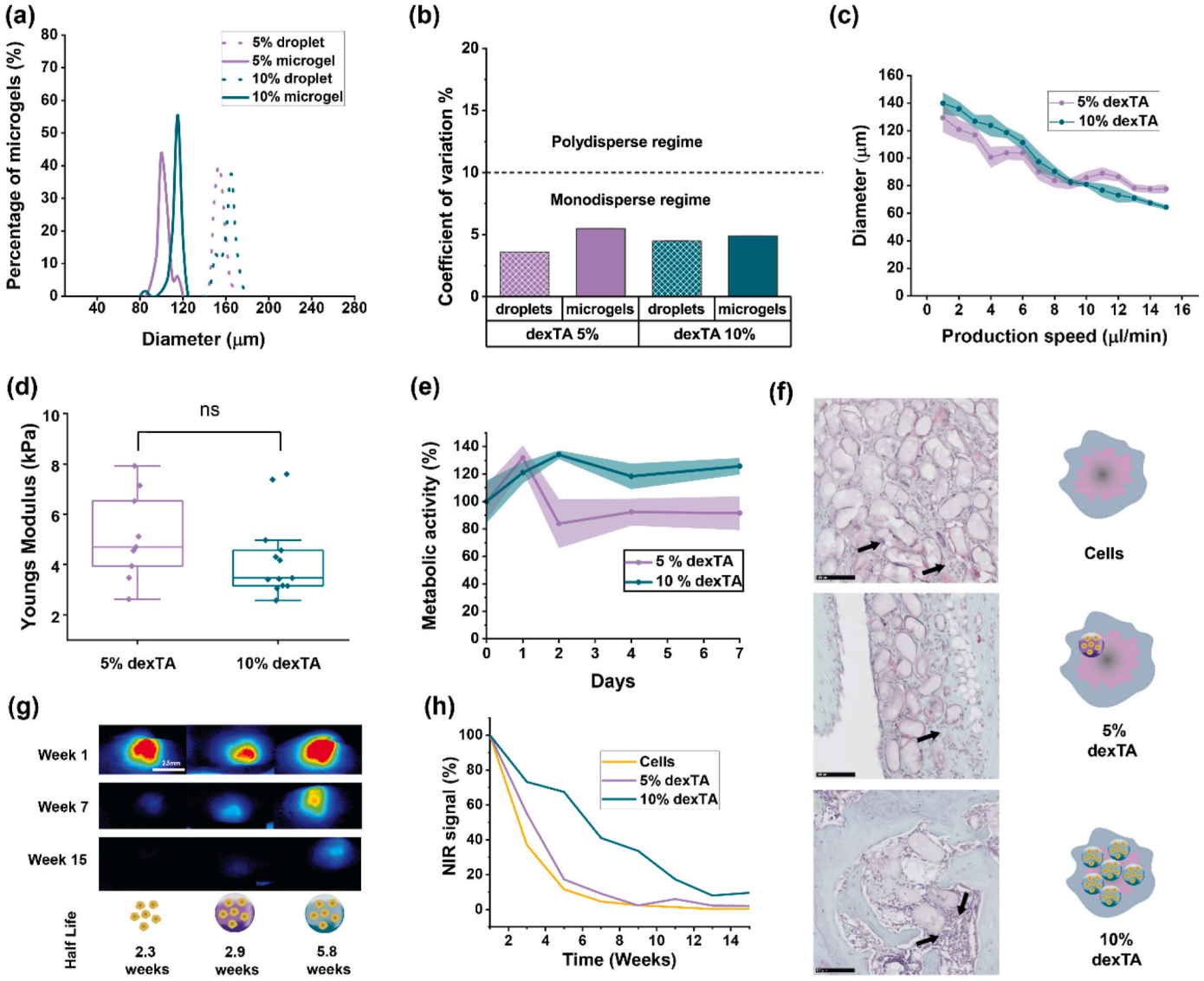

Fig. 2. Material concentration determines the retention time of intra-articularly injected MSC-laden microgels. **(a)** The diameter of 5w/v% or 10w/v% dexTA droplets and microgels was quantified based on image analysis of brightfield micrographs ($n \geq 25$). **(b)** Coefficient of variation of microgels diameter was calculated for 5w/v% or 10w/v% dexTA droplets and microgels ($n \geq 25$). **(c)** Diameter of microgels composed of 5w/v% or 10w/v% dexTA plotted as a function over production speed based on brightfield micrograph quantification ($n \geq 25$). **(d)** Young's modulus of 5w/v% dexTA or 10w/v% dexTA microgels as measured with interferometry-based nanoindentation ($n \geq 9$). **(e)** Metabolic activity of microencapsulated MSCs during seven days of culture ($n \geq 25$). **(f)** Histological sections of the articular rat joints injected with MSCs, MSCs microencapsulated in 5w/v% dexTA, and MSCs microencapsulated in 10w/v% dexTA after 15 weeks of injection ($n = 12$). **(g)** Representative near-infrared images of rat knees injected with near-infrared labeled MSCs that were non-encapsulated or microencapsulated in either 5w/v% dexTA or 10w/v% dexTA microgels for up to 15 weeks ($n = 12$). The scale bar equals 2.5 mm. **(h)** Near-infrared signal percentage of intra-articularly injected near-infrared labeled MSCs as a function of time (15 weeks) ($n = 12$). Graphical data is represented as mean ± standard deviation. Statistical significance was determined by one-way ANOVA (*$p < 0.05$).

polymer concentration affects the retention of microencapsulated stem cells following in vivo implantation.

2.3. Material composition determines biodistribution and retention of MSC-laden microgels in OA-induced joints

Although we demonstrated that polymer content potently affected microgel retention time, it remained unknown whether material composition also affected the retention time of MSC-laden microgels. Specifically, while it is widely known that changes in material composition can alter the mechanical stability, degradation rate, or function of encapsulated cells [49], the characterization and utilization of such material variation have remained unexplored for intra-articular injected systems. To this end, 10w/v% dexTA and 10w/v% dexHATA composed of (5 w/v% dexTA and 5 w/v% HATA) microgels were produced and injected into an OA-induced rat model (Fig. 3a). Biodistribution of

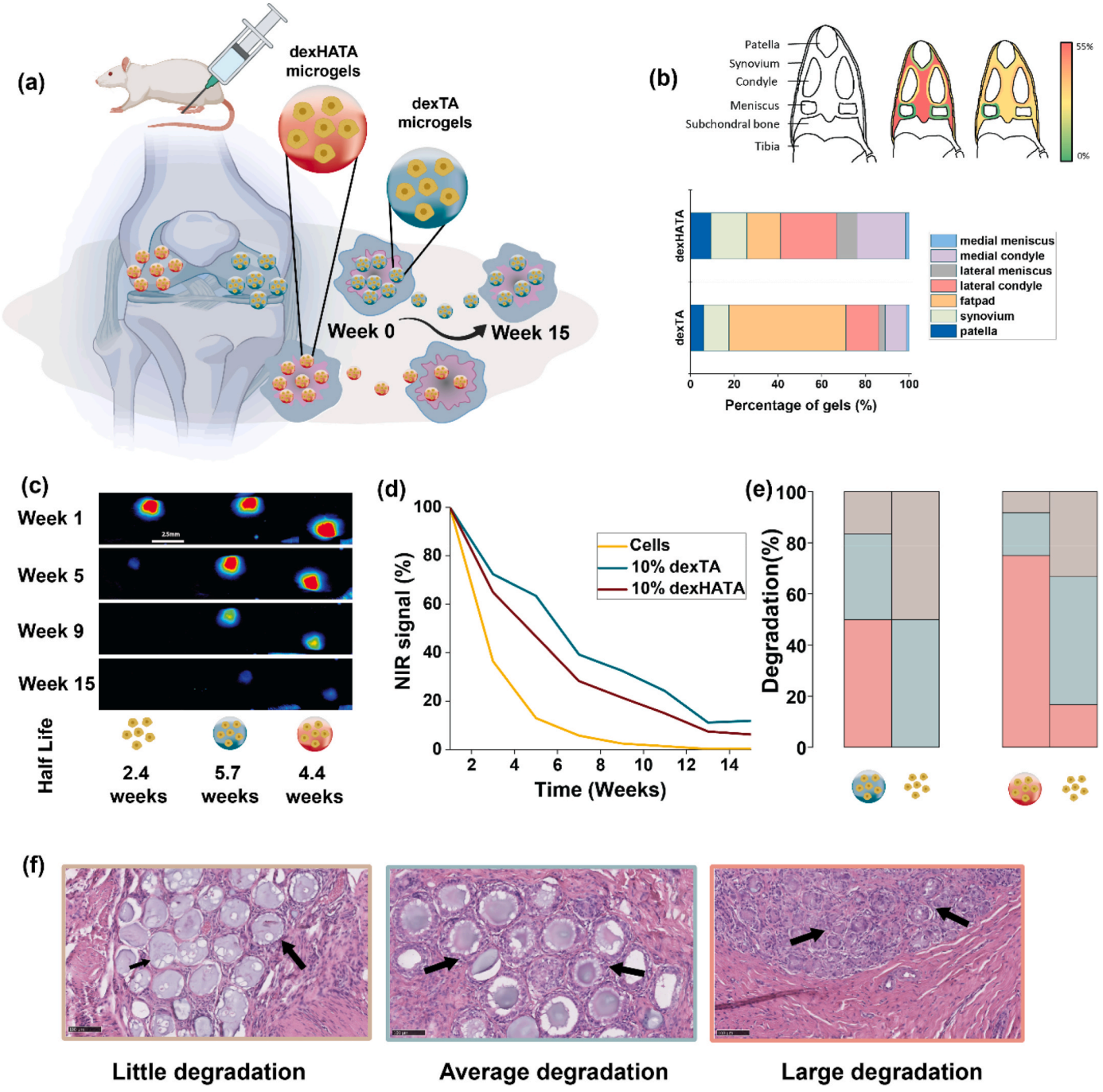

Fig. 3. Material composition determines biodistribution and degradation rate of intra-articularly injected MSC-laden microgels. **(a)** Schematical representation of MSC microencapsulated within dexTA and dexHATA microgels that were injected into rat knee joints with damage-induced cartilage degeneration and analyzed after 15 weeks. **(b)** Percentage distribution of microgels residing in the distinct tissues from histological sections of rat knees (n = 12). **(c)** Representative near-infrared images of rat knees injected with near-infrared labeled MSCs in 10w/v% dexTA or 10w/v% dexHATA microgels for 15 weeks (n = 12). The scale bar equals 2.5 mm. **(d)** Near-infrared signal was quantified and depicted as a percentage of detectable MSCs as a function of time for 15 weeks (n = 12). **(e)** Degradation percentage of 10w/v% dexTA and 10w/v% dexHATA microgels after 15 weeks of injection intra-articulary (n = 12). **(f)** Histological sections representing the various forms of degradation of microgels post 15 weeks post-injection (n = 12).

injected MSC-laden microgels was investigated using (semi-)quantification of histological sections of the entire joints 15 weeks post intra-articular injection. This analysis is relevant as all previous studies focussed solely on the therapeutic effects [50,51], but none have investigated the localized biodistribution at injected site, which could aid in the identification of areas of therapeutic action as well as potential adverse effects. We observed that MSC-laden microgels were present in other tissue than the synovial fluid. While dexTA microgels were predominantly located in the fat pad, dexHATA microgels were more evenly distributed throughout the various joint tissues (Fig. 3b). Whole animal near-infrared imaging of microencapsulated fluorescently-labeled MSCs in microgels was still detectable for both types of polymer 15 weeks post intra-articular injection, while non-encapsulated cells were already mostly cleared 5 weeks post-injection (Fig. 3c). Fluorescence quantification of the near-infrared signals over time suggested that dexTA might offer slightly longer retention of MSCs than dexHATA, (Fig. 3d). This small yet consistent difference might be explained based on the potential degradation rates of dexTA and dexHATA, as MSCs and/or various joint tissues are known to secrete hyaluronidase [52,53] that could potentially degrade hyaluronic acid. Indeed, high-resolution histological analysis corroborated the more intense degradation of dexHATA microgels as compared to dexTA microgels, especially when encapsulating MSCs (Fig. 3e). Together, this demonstrated that biomaterial selection could be used to steer the intra-articular biodistribution of injected microgels, which could potentially have significant implications as distinct joint tissues (e.g., infrapatellar fat pad and synovial membrane) are known as key players that contribute to OA pathophysiology via distinct mechanisms [54]. This form of passive biomaterial-driven enrichment in biodistributions is anticipated as a novel tool to gain further control over locally distinct therapeutic benefits.

2.4. *Whole blood secretomes are altered distinctly for dexTA and dexHATA microgels*

To further investigate the material-dependent inflammatory effects of the microgel formulations, we investigated a broad panel of pro-inflammatory and anti-inflammatory cytokines and chemokines using Luminex multiplex assay after incubation of dexTA and dexHATA microgels with whole blood (Fig. 4a). We prepared a library of interleukins family comprising (IL-6, IL-13, IL-10, IL-4, IL-1b, IL-12) and tumor necrosis factor (TNFα) which contribute a major role in disturbing the balance between anabolic and catabolic process [55,56]. Additionally, proteases contribute to degrading extracellular matrix proteins and proteoglycans like MMPs and TIMPs [57]. CXCL10 expression, since its association with cartilage destruction, and growth factors (VEGF, HGF, PDGF) which contribute to decrease the effects of catabolic proteases like matrix metalloproteinases and complement factor activation C5a [58]. Heatmap representations of various secreted factors for the two compositions of microgels (e.g., dexTA and dexHATA) are presented in Fig. 4b. The pro-inflammatory factor TNF was upregulated at substantially higher levels in dexHATA microgels than in dexTA microgels (Fig. 4c). This suggested that the polymer choice to produce microgels could potentially shift the balance of inflammation, and thus potentially affect the homeostasis of the injected area. Of note, both microgels induced higher levels of pro-inflammatory cytokines, presumably via a foreign body response, with for example IL-6 being increased by both types of microgels at similar levels (Fig. 4d). Pro-inflammatory behavior often coincides with matrix remodeling via altered expression levels of matrix-degrading proteases by shifting the balance between matrix metalloproteinases (MMPs) and tissue inhibitors of metalloproteinases (TIMPs) [59]. A non-significant trend was observed for higher expression of MMP-1 by the more pro-inflammatory dexHATA microgels (Fig. 4e), and higher expression of TIMP-1 by the relatively more anti-inflammatory dexTA microgels (Fig. 4f). Interestingly, despite these observations, the secreted level of MCP-1, which is associated with the cartilage degradation process, was significantly lower in the dexHATA conditions than in dexTA conditions (Fig. 4g). Similarly, expression levels of CXCL10, which is known to associate with the cartilage destruction process following post-traumatic injury [60], were also significantly lower in dexHATA conditions than in dexTA conditions (Fig. 4h). Collectively the multiplex profiling indicated that both tested micromaterials induced a mild inflammatory response in blood, presumably owing to foreign body response, with dexHATA associating with reduced levels of proteins known to associate with cartilage destructive processes. Based on these observations, we speculated on the hypothesis that the distinct microgels could have distinct outcomes in terms of cartilage protection and cartilage degeneration in vivo.

2.5. *Intra-articular injection of MSC-laden microgels influence cartilage degeneration in a material-dependent manner*

OA was induced in rats by using a high-fat diet for 13 weeks followed by a cartilage groove surgery as previously described. The rationale behind choosing the model is the existence of an obesity-related phenotype of osteoarthritis in which low-grade inflammation and a disturbed metabolic profile play a role [61]. Previous studies proved that high-fat diet induces increased OA occurrence in knee. Moreover, it was proven that mechanical induction via groove surgery leads to cartilage degeneration [62]. The high-fat condition in combination with mechanical cartilage damage resulted in a clear significant progression of the osteoarthritic features, with increased synovitis and multiple large osteophytes. Hence, it was evident that a metabolic disbalance due to a high-fat diet increases joint inflammation with cartilage degeneration [63]. The dysmetabolic state clearly accelerates progression of osteoarthritis upon surgically induced cartilage damage. Hence, MSC-laden microgels of dexTA or dexHATA were intra-articularly injected directly post-surgery (Fig. 5a). Intra-articular injections of non-encapsulated MSCs, non-encapsulated MSCs mixed with empty microgels, and saline were used as controls. Eleven weeks after injection, histological analysis revealed that MSC-laden microgels that were injected into the intra-articular region, the microgels residing in Hoffa's Fatpad were surrounded by a massive influx of cells that morphologically resembled multinucleated giant cells and were positive for CD68 indicating a monocytic origin (S4). However, iNOS production by these cells surrounding the microgels was minimal (S3). To gain deeper insights into the health status of the rat joints, histological sections of the joints were analyzed using the OARSI cartilage degeneration scoring system. First, we evaluated the cartilage matrix loss width post-treatment with microgels. In line with the literature, intra-articular injection of non-encapsulated MSCs resulted in less cartilage degeneration as compared to saline injections, which confirmed the potential therapeutic nature of the injected MSCs [64,65]. Microgels of dexHATA showed a significantly reduced matrix loss width as compared to dexTA microgels (Fig. 5b). Average matrix loss was lower in injected microencapsulated MSC than in injections containing both non-encapsulated cells and a mixture of cells and empty microgels for both dexTA and dexHATA, however, this trend did not reach statistical significance. In line with this observation, a material dependency in terms of cartilage degeneration score was observed (Fig. 5c). Specifically, while encapsulating MSCs in dexHATA microgels, they consistently performed better in terms of reducing cartilage matrix loss, cartilage damage, and cartilage degeneration, microencapsulation of MSCs in dexTA performed equal or worse than non-encapsulated MSCs. This effect of material dependency was also consistent when analyzing the percentage of zero matrix loss of cartilage (Fig. 5d). MSCs microencapsulated in dexTA offered no clear therapeutic benefits. However, regardless of the chosen biomaterial, MSCs encapsulated within microgels consistently performed better than non-encapsulated MSC that were co-injected with acellular microgels, which confirmed the added therapeutic benefit of microencapsulating MSCs. Interestingly, non-encapsulated MSCs that were co-injected with acellular dexHATA microgels still outperformed

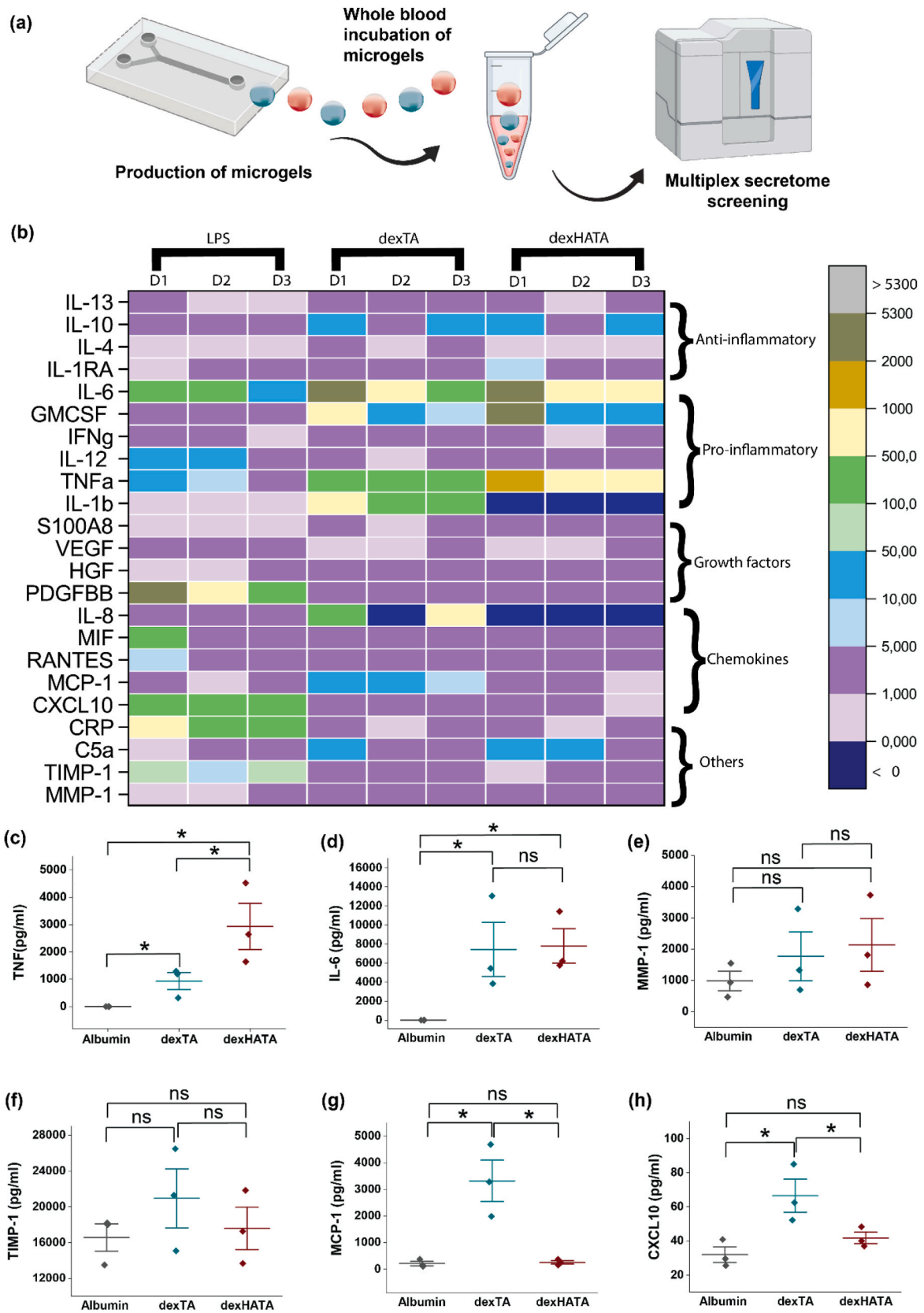

Fig. 4. Multiplexed ELISA analyses of the whole blood secretome following incubation with either dexTA or dexHATA microgels. **(a)** Schematic illustration of the production of microgels followed by whole blood incubation for 2 h and multiplexing the secretomes from the plasma. **(b)** Heatmap of normalized values of various secreted molecules when whole blood from 3 donors is exposed to LPS, 10w/v% dexTA microgels, or 10w/v% dexHATA microgels, with Albumin exposure being used as a negative control for data normalization. Quantitative data as well as the average secreted levels of **(c)** TNF-α, **(d)** IL-6, **(e)** MMP-1, **(f)** TIMP-1, **(g)** MCP-1, **(h)** CXCL10 all expressed as (pg/ml). Graphical data is represented as mean ± standard deviation (n = 3) independent samples for each condition. Statistical significance was determined by Wilcoxon signed-rank test(*$p < 0.05$).

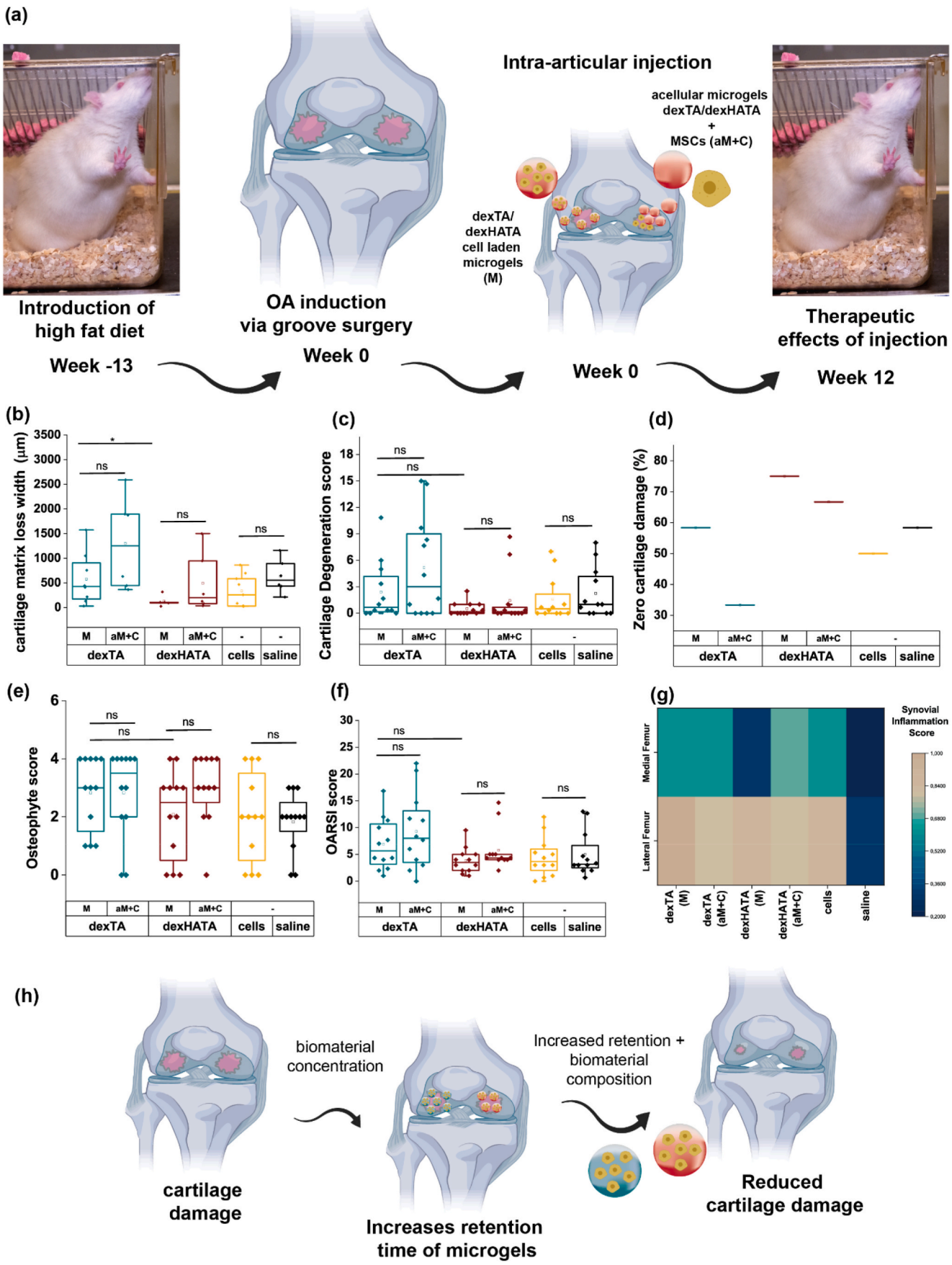

(caption on next page)

Fig. 5. Material-dependent reduction of cartilage damage following intra-articular injection of MSC-laden microgels in a low-grade inflammatory OA model. **(a)** Schematic depiction of the study's design in which rats were put on a pre-fat diet for 13 weeks, followed by intra-articular injections, followed by analysis of therapeutic effects post 12 weeks after injection. Histological sections were analyzed for **(b)** cartilage matrix loss width, **(c)** cartilage degeneration score, **(d)** zero matrix loss in percentage, **(e)** osteophytes score of medial tibia plateau, **(f)** total OARSI score including cartilage degeneration, osteophyte formation, and synovial inflammation for all treatment groups, and **(g)** synovial inflammation score for the lateral and medial femur (n = 12). **(h)** Stem cell-laden microgel's retention capability and therapeutic behavior are based on biomaterial composition and concentration. Data are represented as mean ± standard deviation. "aM + C" represents acellular microgels and non-encapsulated MSCs injected together, "M" represents MSCs encapsulated in respective dexTA or dexHATA microgels. "Cells" denote only MSCs being injected. Statistical significance was determined by one-way ANOVA (*$p < 0.05$).

non-encapsulated MSCs injections, which might suggest that the injection of dexHATA microgels might also offer a therapeutic benefit by itself.

2.6. MSC-laden microgels reduced cartilage damage but did not affect deterioration of other joint tissues

Mitigation of cartilage damage via (non-)encapsulated MSC injection has been reported [66,67], and we here demonstrated that this damage reduction can be augmented in a material-dependent manner by injecting MSC-laden microgels. However, osteoarthritis is a whole joint disease and the therapeutic effects of intra-articularly injected MSCs on non-cartilaginous tissues have rarely been studied. We therefore aimed to determine other clinical indicators that report on joint health such as osteophyte formation and synovial inflammation [68]. Although MSC injections were effective in preventing cartilage damage, none of the investigated treatments observably affected osteophyte formation (Fig. 5e). In contrast, the synovial inflammation score was adversely affected by the injection of MSCs as well as microencapsulated MSCs (Fig. 5f). It is assumed that this adverse effect was caused by the stimulation of sub-synovial tissue proliferation, which results in the thickening of the synovial membrane. We determined that these adverse effects were location-specific as the synovial membrane proximal to the tibia was consistently more affected, while the synovial membrane proximal to the femur was consistently less affected. Moreover, the lateral side was more affected than the medial side of the femur. Based on these observations, the complete OARSI score, which is based on the sum of the cartilage degeneration, osteophyte, and synovial inflammation score, was calculated (Fig. 5g). Specifically, MSC-laden dexHATA microgels outperformed MSC-laden dexTA microgels thus corroborating the material-dependent effect, which was explained by a material-dependent effect on preventing cartilage damage. Interestingly, we observed two subpopulations among treatment groups: a population where the meniscus remained in the correct anatomic location between the lower and the upper leg, and another population where the meniscus was mostly laterally displaced preventing it from offering its natural cushioning effect to the joint (Fig. S5). The two subpopulations differed strongly in their treatment outcome. While the lateral meniscal displaced subpopulation was associated with virtually no reduction of cartilage damage, the subpopulation with a correctly placed meniscus demonstrated excellent reduction of cartilage damage following intra-articular injection of MSC-laden microgels (Fig. S6). However, the articular motion of the joint could be affected by injected micro materials properties at the site of injection, which could potentially affect the distribution pattern of the injected micromaterials. Although, to confirm such a hypothesis further experimental validation and investigation are required. In summary, MSC-laden microgels can potently mitigate cartilage degradation thereby limiting matrix loss and cartilage degeneration in a material-dependent manner in a setting where there is no meniscal displacement.

3. Conclusion

Our study investigated the material-dependent effect of microencapsulated MSC on stem cell retention and subsequent therapeutic effect in induced OA rat models. To this end, we established a straightforward MSC microencapsulation method based on flow-focus microdroplet generation of enzymatically crosslinking MSC-laden bioink. When implanted, the MSC-laden microgels facilitated enhanced retention at the injury site in a material-dependent manner. Specifically, both polymer type and polymer concentration played a key role in determining the retention time of MSCs when injected intra-articularly. Microgels made of dexHATA offered broader biodistribution within the joint and offered a reduction of cartilage degeneration as compared to MSC-laden dexTA microgels and non-encapsulated MSCs. However, the integration of microgels into the synovial membrane is associated with the upregulation of pro-inflammatory factors, which could potentially be mitigated using anti-inflammatory coatings or material formulations. Indeed, using injectable microgel systems that were distinct in either their polymer concentration or type of polymer strongly influenced retention duration, inflammation, and therapeutic outcome. Hence, designing instructive microgels for the microencapsulation of MSCs and other cells can facilitate enhanced long-lasting therapeutic effects and modulate disease progression for osteoarthritis and potentially other pathologies.

4. Materials and methods

4.1. Stem cell isolation and culture

MSCs were isolated from dissected femurs of 12 weeks old male Wistar rats after euthanizing the rats with CO_2. Femurs were placed in sterile PBS with 200 U/ml penicillin and 2 mg/ml streptomycin (Gibco, 15140) for 15 min. The femoral head and condyles were removed, and the bone marrow was flushed from the bones using a serum-free culture medium. The culture medium consisted of α-MEM (Life-Technologies) supplemented with 100 U/ml penicillin, 100 μg/ml streptomycin (Gibco), 2 mM glutamax (Gibco), 0.2 mM L-ascorbic-acid-2-phosphate (ASAP, Gibco), and 10% fetal bovine serum (FBS, Gibco)s. All experiments in this study used primary rat MSCs at passage four, and cells were kept in a humidified environment with 5% CO_2 at 37 °C.

4.2. Microgel production

Dextran conjugated with tyramine moieties (DS 10%) and hyaluronic acid conjugated with both tyramine moieties (DS 3.4%) was synthesized as described previously [69]. Microgels were produced using a droplet-generating microfluidic device that was fabricated via polymerization of PDMS on silicon wafers patterned using standard photolithography, and operated in flow focus mode. In short, MSC-laden microgels were produced with either dexTA (10w/v%) or a 1:1 mixture of dexTA (5w/v%) and HATA (5w/v%) to form dexHATA (10w/v%) as polymer precursor that was dissolved in PBS, which contained $2*10^7$ cells/ml. Polymer solutions with cells were on-chip mixed with H_2O_2 and HRP and co-flown with an oil phase composed of Hexadecane and 1% Span80, with a polymer-to-oil ratio of 1:7. The final concentrations of 14.25 U/ml HRP, 0.535 g/l of H_2O_2, and 8% OptiPrep were used for all experiments unless mentioned otherwise. MSC-laden microgels were collected in a culture medium and filtered through a 40 μm cell strainer directly before microencapsulation. Acellular microgels were produced following the same aforementioned procedure, but without having added cells into the aqueous phase.

4.3. Mechanical characterization of acellular microgels

Microgel size was characterized using brightfield images and quantified using ImageJ software. The surface morphology of microgels was visualized using high-resolution scanning electron microscopy on microgels that were dehydrated in graded ethanol series (70–100%), critical point dried, gold-sputtered for 60 s (Cressington) and imaged with an acceleration voltage of 10 kV (Zeiss-Merlin HR-SEM). The Young's modulus of microgels was determined based on load-indentation curves acquired via interferometry-based optical fiber-top nanoindentation, with an indentation depth of two μm for 1 s (approach and retraction time of 2 s) applying a Hertzian model using a probe of stiffness 0.025 N/m and radius of 9.5 μm (Pavone, Optics11).

4.4. Cell behavior in vitro

The viability and metabolic activity of MSCs in cell-laden microgels were analyzed using live/dead assay and presto blue assay, respectively. Live/dead assay was performed 3 h post-encapsulation with 2 μM calcein AM (live) and 4 μM EthD-1 (dead) and quantified using ImageJ software. Presto Blue experiments were performed 3 h post-encapsulation and at indicated time-intervals for up to 28 days. After 28 days, MSC-laden microgels were fixated in 10% formalin and permeabilized for 10 min in 0.1% Triton-X100, stained for 30 min at room temperature in a mixture of 4 μM EthD-1, 2.5 U ml-1 phalloidin-AF488, and 1 mg l-1 DAPI in PBS, visualized using fluorescent confocal microscopy and processed using ImageJ software.

4.5. Multiplex & ELISA

Blood from three human donors was obtained via the Mini-donor Service at the University Medical Centre (Anonymous). All donors are healthy volunteers that gave written informed consent following the declaration of Helsinki. Briefly, 40 μl of microgels were incubated in 100 μl of blood, and 400 μl RPMI (Gibco). A positive (LPS 1 μg/ml) and negative control (microgels in RPMI medium containing 1 w/w % human serum albumin (Sigma)) were also incubated with blood and culture medium. After 24 h at 37 C°, mixtures were spun down at 1500 g and 4 °C for 10 min), and the supernatant plasma was frozen at −80 C° for multiplex and ELISA analysis. A broad panel of pro and anti-inflammatory cytokine and chemokine libraries was established to analyze the response of the microgels to blood [70].

4.6. Animal experiments

The (Anonymous) University Medical Ethical Committee for animal studies approved the performed studies (AVD 115002016688). 12-week-old male Wistar rats were housed with two animals per cage at a 12h:12h day/night cycle. All rats were randomly assigned to their respective group, afterward ensuring that all groups had an equal weight distribution.

4.7. Retention time study

To determine the intra-articular retention of injected microgels over time, 12 rats were assigned to a microgel group and a control group. Rats in the microgel group had 30 μl of dexTA microgels intra-articularly injected in one knee, and 30 μl of dexHATA microgels in their contralateral knee. These microgels contained $0.5*10^6$ near-infrared labeled MSCs (Invitrogen DIR'; DilC18(7)). Rats in the control group had labeled cells injected in one knee, and saline in the contralateral knee. Bi-weekly NIR-scans (Pearl) were performed under anesthesia (isofluorane: 1–1.5%, dexdomitor: 15–50 μg/kg). After 15 weeks, rats were euthanized using aorta punction, and the knees were collected for histopathological analysis. The retention half-life times were calculated using an exponential fit on the median of six data points (y = -LN(50-Y0/A1) *t1), which is associated with an $R^2 = 0.97$ for dexTA, and a $R^2 = 0.99$ for both dexHATA and non-encapsulated cells.

4.8. Therapeutic effects in rat OA model

To determine the therapeutic effects, cell-laden microgels were intra-articularly injected into the knee joints of a rat osteoarthritis model. Thirty-six rats were randomly assigned to one of three groups and fed a high-fat diet (HF diet) ad libitum of which 60% of the kcal was derived from fat (D12492i, 5.2 kcal/g, Research Diets Inc., NJ) and given free access to water. Twelve weeks after randomization, groove surgery was performed under isoflurane anesthesia (3–4%), as described previously [62]. Directly after surgery, all animals received analgesia (buprenorphine: 0.01–0.05 mg/kg) and were allowed to move freely. One week later, rats were anesthetized and intra-articularly injected in their knee joints with 30 μl of dexTA or dexHATA microgels encapsulating $0.5*10^6$ MSCs. The contralateral control consisted of a mixture of 30 μl microgels and $0.5*10^6$ non-encapsulated MSCs. Directly following intra-articular injection, rats received analgesia and were allowed to move freely. At the endpoint, all animals were euthanized and 18 of the 36 rats were fasted and used for metabolic analysis 18 rats were fasted for 12 h and euthanized using aorta punction. The other 18 rats did not fast and were not used for metabolic analysis. To investigate osteophyte formation, micro-computed tomography (μ-CT) scans were made of all knees (Quantum FX m-CT scanner, PerkinElmer, MA). Specifically, two scans were made: one before treatment and one at the endpoint of the experiment. The μ-CT scans were made using a Quantum FX micro-CT scanner (Caliper Life Sciences, PerkinElmer, Waltham, USA). Both hind limbs were positioned in extension and knee joints were scanned at an isotropic voxel size of 42 μm, voltage of 90 kV, current of 180 μA, and a field of view of 21 mm.

4.9. Immunohistochemistry

The collected knees were immersed in 10% formalin for one week, decalcified using 0.5 M EDTA for 6 weeks, embedded in paraffin, and cut into 5 μm thin slices at 200 μm intervals. These tissue sections were then stained for histological analysis. For the degradation analysis, slides containing Hoffa's Fatpad were rehydrated and stained with hematoxylin (Sigma-GHS332) for 5 min, and Eosin-Y (Sigma-HT110132) for 30 s. We qualitatively scored the remnants of the microgels still residing in the fatpad as little, average, or largely degraded, based on their morphology. For the localization analysis, all microgels at the different locations in the knee were quantified, and normalized to the total gel area in the image. Immunostainings for CD68 and iNOS were performed by antigen retrieval with pepsin (Sigma, 5000U/ml, 30 min, 37C°), blocking with 0.3% H_2O_2 for 10 min, and 5 w/v % PBS-BSA in PBS for 15 min. CD68 & iNOS antibodies (Abcam ab31630), 1:250 and (Santa Cruz sc7271), 1:100 were incubated for 1 h at room temperature. After washing, the goat-*anti*-mouse secondary antibody conjugated to HRP (Agilent P0447) was incubated for 1 h at room temperature, and the staining was visualized using DAB (Abcam ab64238). For the determination of the OARSI scoring, slides of the load-bearing areas of the joint were rehydrated, stained with hematoxylin, fast green (Gill #3, 0.001 w/v %) for 5 min, and safranin O (0.1w/v%) for 10 min. Stained histological sections were imaged (Hamamatsu Nanozoomer), and analyzed on OARSI score according to the gold standard method [24].

4.10. Statistical analysis

All graphical data were represented as mean ± standard deviation. Statistical Analyses were performed using OriginPro 2019b. Statistical significance was represented as "*" for $p > 0.05$ and "ns" for not significant data.

Credit author statement

CJ,LK,MK,JL: Conceptualization, Methodology, Writing-Reviewing and Editing. NK,KW,MK,MB,BZ,BL,SK,HW: Methodology, Data curation.MK and JL Funding.

Declaration of competing interest

The authors declare that they have no known competing financial interests or personal relationships that could have appeared to influence the work reported in this paper.

Data availability

Data will be made available on request.

Acknowledgement

MK acknowledges Europees Fonds voor Regionale Ontwikkeling (00392), and the Dutch Arthritis Foundation (#LLP-25). JL acknowledges financial support from the Innovative Research Incentives Scheme Vidi award (#17522) and the European Research Council(ERC, Starting Grant, #759425).

Appendix A. Supplementary data

Supplementary data to this article can be found online at https://doi.org/10.1016/j.mtbio.2023.100791.

References

[1] M. Chopp, Y. Li, Treatment of neural injury with marrow stromal cells, Lancet Neurol. 1 (2) (2002) 92–100.
[2] E.J. Oh, et al., In vivo migration of mesenchymal stem cells to burn injury sites and their therapeutic effects in a living mouse model, J. Contr. Release 279 (2018) 79–88.
[3] K.C. Rustad, G.C. Gurtner, Mesenchymal stem cells home to sites of injury and inflammation, Adv. Wound Care 1 (4) (2012) 147–152.
[4] S. Regmi, et al., Mesenchymal stem cell therapy for the treatment of inflammatory diseases: challenges, opportunities, and future perspectives, Eur. J. Cell Biol. 98 (5) (2019), 151041.
[5] J. Bashir, et al., Mesenchymal stem cell therapies in the treatment of Musculoskeletal diseases, PM&R 6 (1) (2014) 61–69.
[6] K. Mayilsamy, et al., Treatment with shCCL20-CCR6 nanodendriplexes and human mesenchymal stem cell therapy improves pathology in mice with repeated traumatic brain injury, Nanomed. Nanotechnol. Biol. Med. 29 (2020), 102247.
[7] M. Mohammadi, et al., Mesenchymal stem cell: a new horizon in cancer gene therapy, Cancer Gene Ther. 23 (9) (2016) 285–286.
[8] A. Mohr, R. Zwacka, The future of mesenchymal stem cell-based therapeutic approaches for cancer – from cells to ghosts, Cancer Lett. 414 (2018) 239–249.
[9] F. Papaccio, et al., Concise review: cancer cells, cancer stem cells, and mesenchymal stem cells: influence in cancer development, STEM CELLS Translational Medicine 6 (12) (2017) 2115–2125.
[10] F. Pittenger Mark, et al., Multilineage potential of adult human mesenchymal stem cells, Science 284 (5411) (1999) 143–147.
[11] M.Á. Brennan, P. Layrolle, D.J. Mooney, Biomaterials functionalized with MSC secreted extracellular vesicles and soluble factors for tissue regeneration, Adv. Funct. Mater. 30 (37) (2020), 1909125.
[12] A. Gebler, O. Zabel, B. Seliger, The immunomodulatory capacity of mesenchymal stem cells, Trends Mol. Med. 18 (2) (2012) 128–134.
[13] K. Tamama, S.S. Kerpedjieva, Acceleration of wound healing by multiple growth factors and cytokines secreted from Multipotential stromal cells/mesenchymal stem cells, Adv. Wound Care 1 (4) (2012) 177–182.
[14] J.A. Kode, et al., Mesenchymal stem cells: immunobiology and role in immunomodulation and tissue regeneration, Cytotherapy 11 (4) (2009) 377–391.
[15] M.K.W. Bittencourt, et al., Allogeneic mesenchymal stem cell transplantation in dogs with Keratoconjunctivitis sicca, Cell Med. 8 (3) (2016) 63–77.
[16] A.J. Poncelet, et al., Although pig allogeneic mesenchymal stem cells are not immunogenic in vitro, intracardiac injection elicits an immune response in vivo, Transplantation 83 (6) (2007).
[17] E.C. Doyle, N.M. Wragg, S.L. Wilson, Intraarticular injection of bone marrow-derived mesenchymal stem cells enhances regeneration in knee osteoarthritis, Knee Surg. Sports Traumatol. Arthrosc. 28 (12) (2020) 3827–3842.
[18] L.J. Sandell, T. Aigner, Articular cartilage and changes in Arthritis: cell biology of osteoarthritis, Arthritis Res. Ther. 3 (2) (2001) 107.
[19] K.E. Kuettner, A.A. Cole, Cartilage degeneration in different human joints, Osteoarthritis Cartilage 13 (2) (2005) 93–103.
[20] J.M. Lamo-Espinosa, et al., Intra-articular injection of two different doses of autologous bone marrow mesenchymal stem cells versus hyaluronic acid in the treatment of knee osteoarthritis: multicenter randomized controlled clinical trial (phase I/II), J. Transl. Med. 14 (1) (2016) 246.
[21] Y.S. Kim, Y.I. Kim, Y.G. Koh, Intra-articular injection of human synovium-derived mesenchymal stem cells in beagles with surgery-induced osteoarthritis, Knee 28 (2021) 159–168.
[22] J.A. Ankrum, J.F. Ong, J.M. Karp, Mesenchymal stem cells: immune evasive, not immune privileged, Nat. Biotechnol. 32 (3) (2014) 252–260.
[23] T. Ahmad, et al., Hybrid-spheroids incorporating ECM like engineered fragmented fibers potentiate stem cell function by improved cell/cell and cell/ECM interactions, Acta Biomater. 64 (2017) 161–175.
[24] M.W. Laschke, M.D. Menger, Life is 3D: boosting spheroid function for tissue engineering, Trends Biotechnol. 35 (2) (2017) 133–144.
[25] M. Kung, et al., The synovial lining and synovial fluid properties after joint arthroplasty, Lubricants 3 (2) (2015) 394–412.
[26] M.M. Coronel, et al., Immunotherapy via PD-L1–presenting biomaterials leads to long-term islet graft survival 6 (35) (2020) eaba5573.
[27] J. Lei, et al., FasL microgels induce immune acceptance of islet allografts in nonhuman primates 8 (19) (2022) eabm9881.
[28] X. Zheng, et al., Microskin-inspired injectable MSC-laden hydrogels for scarless wound healing with hair follicles, Adv. Healthcare Mater. 9 (10) (2020), 2000041.
[29] S.-B. Han, et al., Mechanical properties of materials for stem cell differentiation, Advanced Biosystems 4 (11) (2020), 2000247.
[30] A.J. Steward, D.J. Kelly, Mechanical regulation of mesenchymal stem cell differentiation, J. Anat. 227 (6) (2015) 717–731.
[31] G. Tian, et al., Cell-free decellularized cartilage extracellular matrix scaffolds combined with interleukin 4 promote osteochondral repair through immunomodulatory macrophages: in vitro and in vivo preclinical study, Acta Biomater. 127 (2021) 131–145.
[32] Q. Feng, et al., Sulfated hyaluronic acid hydrogels with retarded degradation and enhanced growth factor retention promote hMSC chondrogenesis and articular cartilage integrity with reduced hypertrophy, Acta Biomater. 53 (2017) 329–342.
[33] J. Mak, et al., Intra-articular injection of synovial mesenchymal stem cells improves cartilage repair in a mouse injury model, Sci. Rep. 6 (1) (2016), 23076.
[34] J. Quintavalla, et al., Fluorescently labeled mesenchymal stem cells (MSCs) maintain multilineage potential and can be detected following implantation into articular cartilage defects, Biomaterials 23 (1) (2002) 109–119.
[35] S. Khatab, et al., MSC encapsulation in alginate microcapsules prolongs survival after intra-articular injection, a longitudinal in vivo cell and bead integrity tracking study, Cell Biol. Toxicol. 36 (6) (2020) 553–570.
[36] P. Aprile, et al., Soft hydrogel environments that facilitate cell spreading and aggregation preferentially support chondrogenesis of adult stem cells, Macromol. Biosci. 22 (6) (2022), 2100365.
[37] S.M. Naqvi, L.M. McNamara, Stem cell Mechanobiology and the role of biomaterials in governing Mechanotransduction and matrix production for tissue regeneration, Front. Bioeng. Biotechnol. 8 (2020), 597661.
[38] Y. Xu, et al., Biomaterials for stem cell engineering and biomanufacturing, Bioact. Mater. 4 (2019) 366–379.
[39] X. Liang, et al., Gelatin methacryloyl-alginate core-shell microcapsules as efficient delivery platforms for prevascularized microtissues in endodontic regeneration, Acta Biomater. 144 (2022) 242–257.
[40] J.M. McKinney, et al., Sodium alginate microencapsulation of human mesenchymal stromal cells modulates paracrine signaling response and enhances efficacy for treatment of established osteoarthritis, Acta Biomater. 141 (2022) 315–332.
[41] A. Luanda, V. Badalamoole, Past, present and future of biomedical applications of dextran-based hydrogels: a review, Int. J. Biol. Macromol. 228 (2023) 794–807.
[42] Matera, D.L., et al., Microengineered 3D pulmonary interstitial mimetics highlight a critical role for matrix degradation in myofibroblast differentiation. Sci. Adv.. 6 (37): p. eabb5069..
[43] S. Henke, et al., Enzymatic crosslinking of polymer conjugates is superior over ionic or UV crosslinking for the on-chip production of cell-laden microgels, Macromol. Biosci. 16 (10) (2016) 1524–1532.
[44] T. Kamperman, et al., Tethering cells via enzymatic oxidative crosslinking enables Mechanotransduction in non-cell-adhesive materials, Adv. Mater. 33 (42) (2021), 2102660.
[45] T. Kamperman, et al., Centering single cells in microgels via delayed crosslinking supports long-term 3D culture by preventing cell escape, Small 13 (22) (2017), 1603711.
[46] J.W.H. Wennink, et al., Injectable hydrogels by enzymatic Co-crosslinking of dextran and hyaluronic acid tyramine conjugates, Macromol. Symp. 309–310 (1) (2011) 213–221.
[47] B. van Loo, et al., Enzymatic outside-in cross-linking enables single-step microcapsule production for high-throughput three-dimensional cell microaggregate formation, Materials Today Bio 6 (2020), 100047.
[48] Y. Lei, et al., Stem cell-recruiting injectable microgels for repairing osteoarthritis, Adv. Funct. Mater. 31 (48) (2021), 2105084.
[49] B. Sharma, et al., Human cartilage repair with a photoreactive adhesive-hydrogel composite, Sci. Transl. Med. 5 (167) (2013), 167ra6-167ra6.
[50] M. Satué, et al., Intra-articularly injected mesenchymal stem cells promote cartilage regeneration, but do not permanently engraft in distant organs, Sci. Rep. 9 (1) (2019), 10153.
[51] L. Scarfe, et al., Non-invasive imaging reveals conditions that impact distribution and persistence of cells after in vivo administration, Stem Cell Res. Ther. 9 (1) (2018) 332.

[52] K. Gwon, E. Kim, G. Tae, Heparin-hyaluronic acid hydrogel in support of cellular activities of 3D encapsulated adipose derived stem cells, Acta Biomater. 49 (2017) 284–295.
[53] C. Gao, et al., VE-cadherin functionalized injectable PAMAM/HA hydrogel promotes endothelial differentiation of hMSCs and vascularization, Appl. Mater. Today 20 (2020), 100690.
[54] M. Favero, et al., Infrapatellar fat pad features in osteoarthritis: a histopathological and molecular study, Rheumatology 56 (10) (2017) 1784–1793.
[55] S. Gabner, et al., Cytokine-induced interleukin-1 receptor antagonist protein expression in genetically engineered equine mesenchymal stem cells for osteoarthritis treatment, J. Gene Med. 20 (5) (2018) e3021.
[56] C. Liu, et al., Cytokines: from clinical significance to quantification, Adv. Sci. 8 (15) (2021), 2004433.
[57] E.-S.E. Mehana, A.F. Khafaga, S.S. El-Blehi, The role of matrix metalloproteinases in osteoarthritis pathogenesis: an updated review, Life Sci. 234 (2019), 116786.
[58] C. Gaissmaier, J.L. Koh, K. Weise, Growth and differentiation factors for cartilage healing and repair, Injury 39 (2008) 88–96, 1, Supplement.
[59] G.H. Yuan, K. Masuko-Hongo, K. Nishioka, Role of chemokines/chemokine receptor systems in cartilage degradation, Drug News Perspect. 14 (10) (2001) 591–600.
[60] B.D. Furman, et al., CXCL10 is upregulated in synovium and cartilage following articular fracture, J. Orthop. Res. 36 (4) (2018) 1220–1227.
[61] T.M. Griffin, F. Guilak, Why is obesity associated with osteoarthritis? Insights from mouse models of obesity, Biorheology 45 (2008) 387–398.
[62] H.M. de Visser, et al., Groove model of tibia-femoral osteoarthritis in the rat, J. Orthop. Res. 35 (3) (2017) 496–505.
[63] H.M. de Visser, et al., Metabolic dysregulation accelerates injury-induced joint degeneration, driven by local inflammation; an in vivo rat study, J. Orthop. Res. 36 (3) (2018) 881–890.
[64] A.T.L. Lam, S. Reuveny, S.K.-W. Oh, Human mesenchymal stem cell therapy for cartilage repair: review on isolation, expansion, and constructs, Stem Cell Res. 44 (2020), 101738.
[65] A. Goldberg, et al., The use of mesenchymal stem cells for cartilage repair and regeneration: a systematic review, J. Orthop. Surg. Res. 12 (1) (2017) 39.
[66] P.K. Gupta, et al., Mesenchymal stem cells for cartilage repair in osteoarthritis, Stem Cell Res. Ther. 3 (4) (2012) 25.
[67] K.B. Lee, et al., Injectable mesenchymal stem cell therapy for large cartilage defects–a porcine model, Stem Cell. 25 (11) (2007) 2964–2971.
[68] N. Gerwin, et al., The OARSI histopathology initiative – recommendations for histological assessments of osteoarthritis in the rat, Osteoarthritis Cartilage 18 (2010) S24–S34.
[69] R. Jin, et al., Enzymatically-crosslinked injectable hydrogels based on biomimetic dextran–hyaluronic acid conjugates for cartilage tissue engineering, Biomaterials 31 (11) (2010) 3103–3113.
[70] J. Paquet, et al., Cytokines profiling by multiplex analysis in experimental arthritis: which pathophysiological relevance for articular versus systemic mediators? Arthritis Res. Ther. 14 (2) (2012) R60.